● RESEARCH ARTICLE

An appropriate level of autophagy reduces emulsified isoflurane-induced apoptosis in fetal neural stem cells

Ze-Yong Yang[1, *, #], Lei Zhou[2, #], Qiong Meng[1], Hong Shi[3], Yuan-Hai Li[2, *]
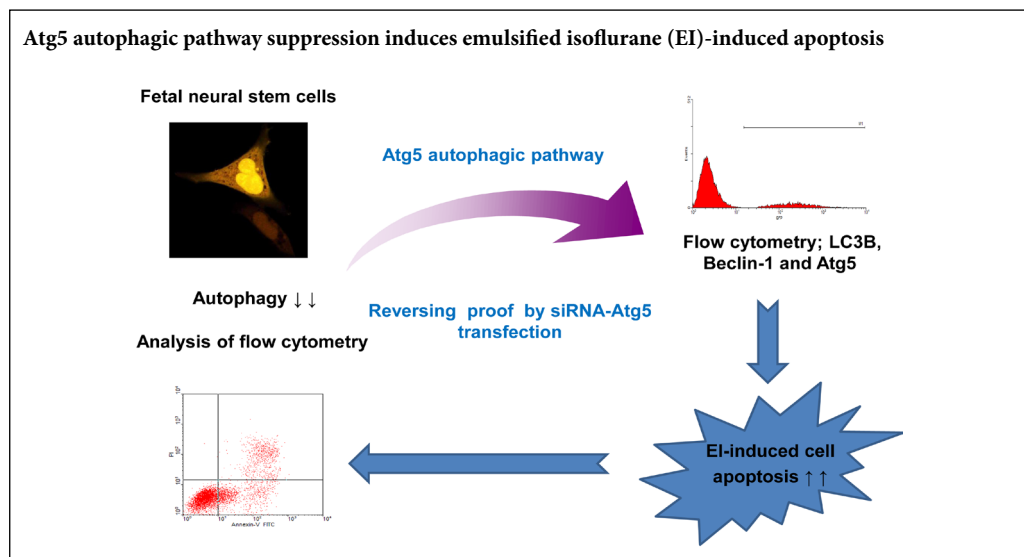
1 Department of Anesthesiology, International Peace Maternity and Child Health Hospital, Shanghai Jiao Tong University School of Medicine, Shanghai Key Laboratory of Embryo Original Disease, Shanghai Municipal Key Clinical Specialty, Shanghai, China
2 Department of Anesthesiology, First Affiliated Hospital of Anhui Medical University, Hefei, Anhui Province, China
3 Department of Anesthesiology, Shanghai Pulmonary Hospital, Tongji University, Shanghai, China

Graphical Abstract

Atg5 autophagic pathway suppression induces emulsified isoflurane (EI)-induced apoptosis

Fetal neural stem cells

Atg5 autophagic pathway

Flow cytometry; LC3B, Beclin-1 and Atg5

Autophagy ↓↓

Reversing proof by siRNA-Atg5 transfection

Analysis of flow cytometry

EI-induced cell apoptosis ↑↑

Abstract

Autophagy plays essential roles in cell survival. However, the functions and regulation of the autophagy-related proteins Atg5, LC3B, and Beclin 1 during anesthetic-induced developmental neurotoxicity remain unclear. This study aimed to understand the autophagy pathways and mechanisms that affect neurotoxicity, induced by the anesthetic emulsified isoflurane, in rat fetal neural stem cells. Fetal neural stem cells were cultured, *in vitro*, and neurotoxicity was induced by emulsified isoflurane treatment. The effects of pretreatment with the autophagy inhibitors 3-methyladenine and bafilomycin and the effects of transfection with small interfering RNA against ATG5 (siRNA-Atg5) were observed. Cell viability was determined using the 3-(4,5-dimethylthiazol-2-yl)-2,5-diphenyltetrazolium bromide assay, and apoptosis was assessed using flow cytometry. Ultrastructural changes were analyzed through transmission electron microscopy. The levels of the autophagy-related proteins LC3B, Beclin 1, Atg5, and P62 and the pro-apoptosis-related protein caspase-3 were analyzed using western blot assay. The inhibition of cell proliferation and that of apoptosis rate increased after treatment with emulsified isoflurane. Autophagolysosomes, monolayer membrane formation due to lysosomal degradation, were observed. The autophagy-related proteins LC3B, Beclin 1, Atg5, and P62 and caspase-3 were upregulated. These results confirm that emulsified isoflurane can induce toxicity and autophagy in fetal neural stem cells. Pre-treatment with 3-methyladenine and bafilomycin increased the apoptosis rate in emulsified isoflurane-treated fetal neural stem cells, which indicated that the complete inhibition of autophagy does not alleviate emulsified isoflurane-induced fetal neural stem cell toxicity. Atg5 expression was decreased significantly by siRNA-Atg5 transfection, and cell proliferation was inhibited. These results verify that the Atg5 autophagy pathway can be regulated to maintain appropriate levels of autophagy, which can inhibit the neurotoxicity induced by emulsified isoflurane anesthetic in fetal neural stem cells.

Key Words: *apoptosis; Atg5; autophagy; emulsified isoflurane; fetal neural stem cells; LC3B; MTT; neurodegenerative; neurotoxicity*

Chinese Library Classification No. *R459.9; R363; R364*

Introduction

Numerous studies have shown that exposure to anesthetics can induce cell apoptosis, leading to synaptic remodeling and modifying of the morphology of the developing brain (Culley et al., 2004; Loepke et al., 2009; Stratmann et al., 2009; Zhao et al., 2010, 2013; Zhu et al., 2010a). Additionally, in humans and animals, anesthetic treatments early in life can induce neurohistopathological changes, cognitive disorders, and the development of learning disabilities (Monk et al., 2008; Kalkman et al., 2009; Wilder et al., 2009; Istaphanous et al., 2013; Zhao et al., 2013). Emulsified isoflurane (EI) is an emulsion formulation of isoflurane, with characteristics of both intravenous and inhalational anesthesia that can be safely used as an intravenous anesthetic (Huang et al., 2014).

Autophagy is a regulated degradative process that facilitates the recycling of cellular components under stress conditions and protects cells from death (Mizushima et al., 2007). Autophagy is involved in non-apoptotic cell death, termed autophagic cell death (Tsujimoto et al., 2005), which has been linked to several neurodegenerative diseases, such as Parkinson's disease, Huntington's disease and Alzheimer's disease (Anglade et al., 1997; Boland et al., 2008; Sarkar et al., 2008; Ciechanover et al., 2015; Menzies et al., 2017; Plaza-Zabala et al., 2017; Switon et al., 2017; Guo et al., 2018; Cerri et al., 2019).

However, the role played by autophagy during EI-induced neurocytotoxicity remains poorly understood. The regulation and functions of autophagy during embryonic neural development are also unclear. In this study, we hypothesized that autophagy decreases the EI-induced apoptosis of fetal neural stem cells (FNSCs), via the Atg5 autophagic pathway, which has been shown to diminish EI-induced neurotoxicity of EI during *in vitro* approaches. This study examined the role played by autophagy in EI-induced disorders.

Materials and Methods

FNSC cultures

Primary FNSCs were purchased from Life Technologies (Carlsbad, CA, USA). The cells were removed from liquid nitrogen storage and immediately transferred to a 37°C water bath, to thaw, which was performed in 2 minutes. The cells were then transferred to a centrifuge tube, and a pre-warmed complete medium (Invitrogen, Carlsbad, CA, USA) was immediately added, to a final volume of 10 mL. After centrifugation, the supernatant was discarded, and cell viability was assessed. Cell viability should be greater than 50%. Cellstart (Invitrogen) was used to treat 25-cm cell culture flasks. Complete medium was added, according to the required cell concentration. The cell culture flasks were placed in a 37°C incubator for 24 hours. The next day, the medium was replaced with the same amount of fresh, pre-warmed, complete medium.

Culture: Cells were cultured using prepared StemProR neural stem cell (NSC) serum-free medium. GlutaMAX™ (5 mL), 2% StemPro® Neural Supplement (10 mL) and epidermal growth factor (10 ng/mL, 0.5 mL) were added to KnockOut™ DMEM/F-12 (483.5 mL), followed by shaking and filtering before storage at 4°C. All reagents were obtained from Invitrogen. Embryonic NSCs, with viability greater than 90%, were seeded at a density of $2–5 \times 10^5$/mL, in 25-cm culture flasks, pre-treated with Cellstart. Cells were incubated 37°C, in a 5% CO_2 environment. After 3–4 days of culture, when the cells reached 70–90% confluence, the cells were passaged. Rat FNSCs could be propagated for 3–5 passages, without differentiation, with more than 85% of cells retaining an undifferentiated phenotype.

Confirmation of FNSCs

After 3–5 passages, cells were washed 3–4 times with washing buffer [phosphate-buffered saline (PBS), containing 8.0 g NaCl, 0.2 g KCl, 1.56 g Na_2HPO_4, and 0.2 g KH_2PO_4], fixed with 6% paraformaldehyde for 30 minutes, and washed again 3–4 times for 2 minutes each time. Then, the cells were treated with a blocking solution for approximately 30 minutes and incubated with the primary antibody, (anti-nestin antibody, 1:200, ab6142, Abcam, Cambridge, UK), at 4°C for 1–2 days, followed by secondary antibody [fluorescein isothiocyanate (FITC)-conjugated anti-mouse IgG] for 37°C, 1 hour. After washing with washing buffer, cell nuclei were stained with 8 µg/L 4′,6-diamidino-2-phenylindole (DAPI). Cells were then washed and observed under a fluorescent microscope.

EI treatment

Cells cultured in the same batch were randomly divided into 9 groups (n = 8 per group). In the normal control group (group N), normal cells were continuously cultured for 12 hours. In the fat emulsion group (group F), intralipid was added to the culture medium, and cells were cultured using the same method as group N. Intralipid® (30%; Huarui Pharmacy, Chengdu, China) was used to dissolve liquid isoflurane (Abbott Laboratories, Queenborough, Kent, UK), and served as the vehicle for the EI suspension preparation. EI (Yichang Humanwell Pharmaceutical Co., Ltd., Hubei, China) was prepared by dissolving liquid isoflurane in 30% intralipid at a 1:11.5 volume ratio, with an 8% isoflurane concentration (v/v). Three different concentrations of EI were added to the culture medium (KnockOut™ DMEM/F-12; Invitrogen): 7.56, 9.52, and 11.48 mM. The following treatment groups were used: 7.56 mM EI (group EI1), 9.52 mM EI (group EI2), EI2 plus autophagy blocker 3-methyladenine (3-MA, group EI2M), EI2 plus autophagy blocker bafilomycin (group EI2B), EI2 plus transfection of small-interfering RNA against Atg5 (siRNA-Atg5, group EI2S), EI2 plus negative-siRNA (group EI2NS), and 11.48 mM EI (group EI3). All concentrations were determined from the results of our preliminary experiments, and the remaining culture steps were the same as those used for group N.

Flow cytometry after EI treatment

After measuring cell viability, cell apoptosis was assessed using flow cytometry, to identify cells in different phases of apoptosis. An Annexin V FITC apoptosis DTEC kit I 100TST (BD Biosciences, Franklin Lakes, NJ, USA) was used to evaluate apoptotic cells. Cells were stained with Annexin V and propidium iodide (PI), fixed in 4% paraformaldehyde, and assessed by flow cytometry (Peng et al., 2008). The sur-

vival rate of FNSCs was quantitatively analyzed by detecting early apoptosis (Annexin V^+/PI^-), late apoptosis/necrosis (Annexin V^+/PI^+), and normal cells (Annexin V^-/PI^-). The apoptotic rate (ratio of Annexin V^+/PI^- + Annexin V^+/PI^+: total number of cells) was measured by flow cytometry (Thermo Scientific, Shanghai, China).

3-(4,5-Dimethylthiazol-2-yl)-2,5-diphenyltetrazolium bromide assay

After EI treatment, cell viability was evaluated using a 3-(4,5-dimethylthiazol-2-yl)-2,5-diphenyltetrazolium bromide (MTT) reduction assay, as previously described (Zhao et al., 2013). Cultured rat FNSCs were plated at 1.5×10^4 cells per well in 96-well plates, and 10 μL MTT (Beyotime, Shanghai, China) was added to each well for 4 hours. The medium was aspirated, and 100 μL dimethyl sulfoxide was added to each well for 10 minutes to dissolve the purple formazan. The samples were quantified spectrophotometrically, at 490 nm, using a microplate reader (SpectraMax® 190, San Diego, CA, USA).

Western blot assay

After assessing cell viability and apoptosis, protein expression was observed by western blot assay. The cells were washed with phosphate-buffered saline. 100 μL RIPA lysis buffer (Cell Signaling Technology, Danvers, MA, USA) was added to each cell well, and after full lysis, all lysate was collected. The lysate was centrifuged at $14,000 \times g$ at 4°C after incubation on ice for 30 minutes, and the supernatant was reserved. After the gel was made, electrophoresis buffer was added and the polymerized gel was placed in the electrophoresis tank. The protein concentration of all protein extracts was adjusted to 6 μg/μL, and an equal volume of 2 × loading buffer was added to each sample to prepare a loading solution. The loading solution was then treated at high temperature to denature the protein, followed by centrifugation at 5000 r/min for 2 minutes, at low temperature. A volume of 15 μL of loading solution was added to each well, and a pre-stained Marker was used as a control well. Electrophoresis was performed at a constant voltage of 80 V for 30 minutes. After the indicator entered the separated adhesive, the voltage was changed to 110 V. Finally, the power was turned off when the indicator reached the bottom and the gel plate was removed. Polyvinylidene fluoride membrane was immersed in methanol for 15 seconds, rinsed, and soaked in transfer buffer solution for 5 minutes. The gel blocks were trimmed and soaked in the transfer buffer for 20 minutes. The gel was transferred onto the membrane at a constant voltage of 100 V for 1 hour, from the negative electrode to the positive electrode. The membrane was sealed with 5% bovine serum albumin blocking buffer at room temperature, approximately 2 hours. The membrane was washed no less than 3 times, for a minimum of 5 minutes. Membranes were incubated overnight at 4°C with specific primary antibodies against caspase-3 (apoptosis-related protein, 1:500, mouse, monoclonal antibody), LC3B (autophagy-related protein, 1:500, mouse, monoclonal antibody), Atg5 (autophagy-related protein, 1:500, rabbit, monoclonal antibody), and Beclin 1 (autophagy-related protein, 1:500, rabbit, monoclonal anti-

body) from Cell Signaling Technology (Danvers, MA, USA), by gently shaking, followed by incubation with the appropriate horseradish peroxidase-conjugated secondary antibodies (1:3000) for 2 hours at room temperature. Glyceraldehyde 3-phosphate dehydrogenase was used as a loading control. Protein expression levels were measured semiquantitatively with Quantity One software (Version 4.6.9, Bio-Rad, Hercules, CA, USA), by calculating the relative expression rates (ratio of target band gray value to reference band gray value).

Measurement of autophagy flux

Cells were incubated for 12 hours after being divided into treatment groups. Autophagy activation in the N, F, and EI2 groups was evaluated by plasmid transfection technology and transmission electron microscopy (JEM 2010, JEOL, Tokyo, Japan). Transmission electron microscopy: The cells were immediately fixed with 2.5% glutaraldehyde, containing 0.1 mol/L sodium cacodylate, and stored at 4°C. The samples were postfixed with 1% osmium tetroxide and dehydrated through graded ethanol (50%, 70%, 90%, and 100%) and propylene oxide series (50%). Epoxy resin was added to pre-labeled embedding plates, and the fixed samples were placed into the resin. The embedding surface was adjusted, the samples were placed in a thermostatic chamber to cure for 2 to 3 days. After embedding, ultrathin (50–60 nm) sections were cut using an ultramicrotome (LKB-I, Rockville, MD, USA). Images were captured with a transmission electron microscope, at 80 kV, after the samples were stained with 3% uranium dioxide acetate and lead citrate. The staining procedure is as follows: a piece of filter paper was laid on the bottom of the dish, moistened with the dye solution and a small piece of clean dental wax was placed on top. The dye was dropped onto the wax, and the plate was quickly covered with dye. The loading net was dyed with either 1–3% acetic acid dioxygen uranium solution or 70% alcohol solution for 20–30 minutes. After washes, the net was generally immersed in a cleaning liquid, using tweezers. After repeated cleaning, the cleaning liquid was removed and the dying net was floated on a droplet, to ensure that the slice was facing down. Lead citrate was prepared from lead nitrate and sodium citrate and dissolved in sodium hydroxide, to obtain a stable, strong, base solution (pH 12). The same methods were used for lead citrate dyeing and washing. Plasmid transfection procedure: The cells were plated at the desired density (50–80%) The required volume of LC3B-FP (Component A) (BacMam 2.0) from Invitrogen (Carlsbad, CA, USA) and LC3B (G120A)-FP (Component B) was calculated, according to the formula indicated in the instruction manual. The LC3B reagents were mixed and added directly to the cells in complete cell medium, followed by gentle mixing. The cells were incubated overnight (≥ 16 hours). The following day, the cells were grouped, according to the required experimental requirements. Each group of cells was observed using confocal microscopy (LSM510, Zeiss, Jena, Germany) 6, 12, and 24 hours after grouping, and fluorescent images were captured. The expression of green fluorescent protein (GFP)-LC3B was quantitatively analyzed using flow cytometry.

EI treatment with autophagy interference

Cultured rate FNSCs (group EI2M) were treated with 10 mM 3-MA, which inhibits the phosphoinositide-3-kinase (PI3K) autophagy pathway, and 25 nM bafilomycin (group EI2B), a specific blocker of vacuolar-type H^+-ATPase, which are both widely used autophagy inhibitors.

siRNA-mediated knockdown

After neurotoxicity experiments, Atg5 gene knockdown was achieved, using small interfering RNA (siRNA) (Gene-Pharma, Shanghai, China). The following siRNAs for Atg5 (GenePharma) were cloned into lentiviral vectors: 5′-GCA TTA AAG CAG CGT ATC-3′ for siAtg5 number 1, 58 bp; 5′-GC ATT AAA GCA GCG TAT C-3′ for siAtg5 number 2, 58 bp and 5′-GCA TTA AAG CAG CGT ATC-3′ for siAtg5 number 3, 59 bp. Lipofectamine 3000 (Life Technologies) transfection reagent was used, as described previously (Seong et al., 2019), in accordance with the manufacturer's instructions. In brief, siRNA for Atg5, or control, scrambled siRNA was diluted into each well of a 6-well plate containing Transfection Medium (Opti-MEM; Invitrogen) and incubated for 5 minutes. In parallel, Lipofectamine was diluted in Transfection Medium (Opti-MEM) at a ratio of 5 μL Lipofectamine 3000 in 245 μL Opti-MEM culture medium. The diluted Lipofectamine reagent and siRNA were mixed and incubated at room temperature for 20 minutes. Cells were cultivated for 24 hours after transfection. Cells were then harvested for further experiments or to confirm knockdown efficiency, via immunoblotting.

Statistical analysis

Data are presented as the mean ± SD. All statistical analyses were performed in Graphpad Prism 5.0 software (GraphPad, Inc., La Jolla, CA, USA). Multigroup comparisons of the measurement data were processed by a one-way analysis of variance followed by Tukey's *post hoc* test. A value of $P < 0.05$ was considered significant.

Results

Immunofluorescence and confirmation of FNSCs

More than 85% of control cells were positively stained for both DAPI and nestin after the third passage, suggesting that the cultured cells were FNSCs (**Figure 1**). DAPI labels nuclei, which appeared blue (**Figure 1A**), and nestin immunocytochemistry was used to identify the cultured cells as FNSCs (**Figure 1B**). Nestin immunoreactivity (red color) appeared primarily in the cytoplasm. Nestin- and DAPI-positive staining indicated the presence of cultured NSCs (**Figure 1C**), providing a foundation for subsequent experiments.

EI-induced apoptosis of FNSCs

EI significantly inhibited the FNSC viability at concentrations greater than 7.56 mM compared with the intralipid control. In groups exposed to EI, cell apoptosis increased compared with control and intralipid-treated cells (**Figure 2A** and **B**). The cell survival rate was determined using an annexin V assay because FITC-annexin V binds to phosphatidylserine during cell apoptosis. The cell apoptosis rates for all EI groups increased compared with those of groups N and F, as measured by the MTT assay ($P < 0.0001$; **Figure 2A** and **B**). The level of caspase-3 was upregulated by EI, in a dose-dependent manner ($P < 0.05$; **Figure 2C**).

Ultrastructural morphology of FNSCs following EI exposure

To determine the mechanism of EI-induced apoptosis in FNSCs, the ultrastructural morphology of cells was examined using electron microscopy following EI treatment for 6, 12, and 24 hours. The results showed that autophagosome formation was significant compared with that in group N (**Figure 3**). Electron microscopy revealed the formation of multivesicular and body-like vesicles, which is a characteristic of autophagosomes, after different durations of EI exposure (**Figure 3**).

EI-induced cell autophagy in FNSCs

LC3B, an autophagy hallmark, increased in the EI-treated groups. Increased P62, Atg5, LC3B, and Beclin-1 levels were detected, as shown in **Figure 4A** and **B**. The formation of LC3 puncta is often observed in cells during autophagic activation. FNSCs were transfected with GFP-LC3 to further evaluate whether EI treatment induced an autophagic response. The GFP fluorescence results showed that EI significantly increased the number of GFP-LC3 puncta (**Figure 4C** and **D**).

Autophagy inhibition increases EI-induced toxicity in FNSCs

To confirm the role played by autophagy during EI-induced neurotoxicity, autophagy in FNSCs was inhibited, using 3-MA, a class III PI3K inhibitor, and bafilomycin A1, which inhibits autophagosome and lysosome fusion. The inhibition of cellular proliferation increased in EI-treated groups increased compared with groups N and F. Moreover, for this inhibition of cellular proliferation, apoptosis rate and expression of caspase-3 increased in the groups EI2M and EI2B compared with those in the EI-treated groups (**Figure 5A** and **B**). Pretreatment with 3-MA inhibited autophagy and significantly increased EI-induced neurotoxicity in FNSCs.

Detection of FNSC apoptosis following EI treatment under autophagy-related gene silencing conditions

Gene silencing, MTT assay, and western blot assay were conducted to test the inhibition of cell survival in the absence of a critical autophagy-related protein. Atg5 protein expression decreased significantly in group EI2S compared with group EI2NS ($P < 0.01$; **Figure 6A** and **B**). FNSC proliferation in group EI2 was increased compared with group F. FNSC proliferation was inhibited in group EI2S compared with group EI2NS, which indicated that autophagy inhibition increased EI-induced apoptosis (**Figure 6C**).

Discussion

In this study, the proliferation of FNSCs was inhibited in group EI2S compared with group EI2NS, indicating that autophagy inhibition increased EI-induced apoptosis. Autophagy has been demonstrated to play an important role in various neurodegenerative disorders, such as Parkinson's
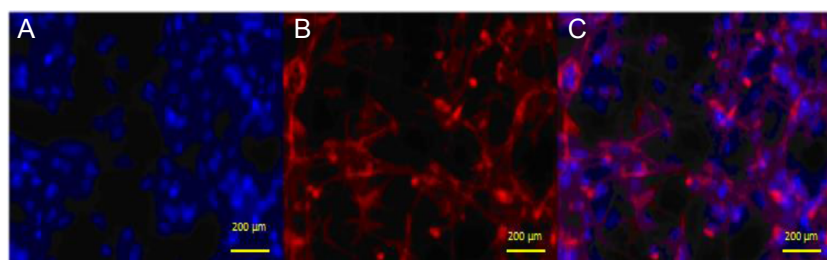
Figure 1 Identification of FNSCs after culturing for 3–5 passages (immunofluorescence staining, using an IN Cell Analyzer 1000; fluorescence microscope). Immunofluorescence detection indicated that the undifferentiated FNSC phenotype was maintained in greater than 85% of cells. (A) DAPI nuclear staining (blue). (B) Immunostained nestin-positive FNSCs (red). (C) Merged image for nestin and DAPI, showing the cultured FNSCs. DAPI: 4′,6-Diamidino-2-phenylindole; FNSCs: fetal neural stem cells. Scale bars: 200 μm.
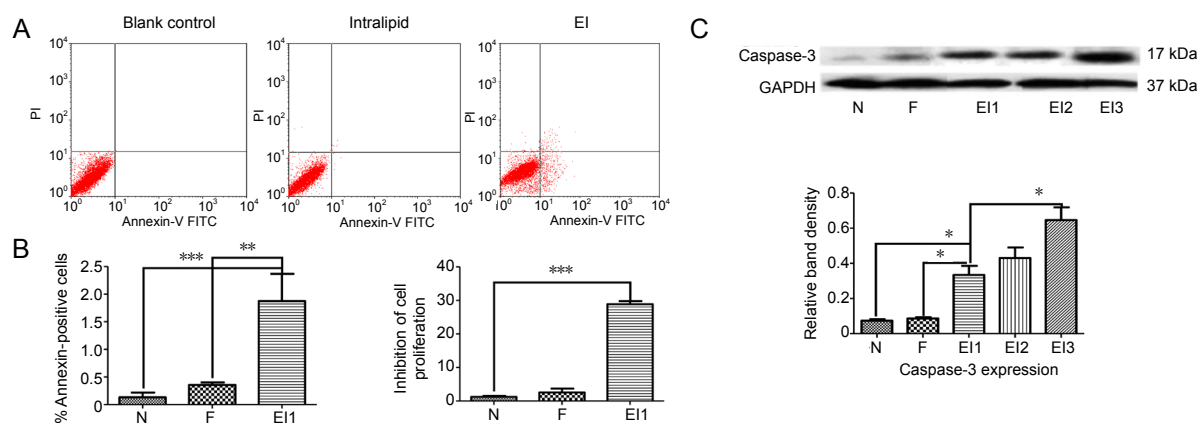
Figure 2 Inhibition of proliferation and caspase-3 levels in fetal neural stem cells.
(A) Cells were treated with EI, cultured for 6 hours, and then cell apoptosis was analyzed by flow cytometry. (B) Annexin V-FITC and PI staining after cells were treated with 9.56 mM EI for 6 hours. The inhibition of cell proliferation increased in the EI1 group. (C) Western blot assay showing the apoptosis-related protein caspase-3 (17 kDa). Cells were treated with different concentrations of EI and cultured for 12 hours. GAPDH (37 kDa) was used as a loading control. All data were derived from the results of three independent experiments. Data are expressed as the mean ± SD ($n = 8$ for each condition; one-way analysis of variance with Tukey's *post hoc* test). *$P < 0.05$, **$P < 0.01$, ***$P < 0.001$. EI1, EI2, EI3: 7.56, 9.52, 11.48 mM EI groups, respectively; F: Fat emulsion group; N: normal control group. EI: Emulsified isoflurane; FITC: fluorescein isothiocyanate; GAPDH: glyceraldehyde-3-phosphate dehydrogenase; PI: propidium iodide.
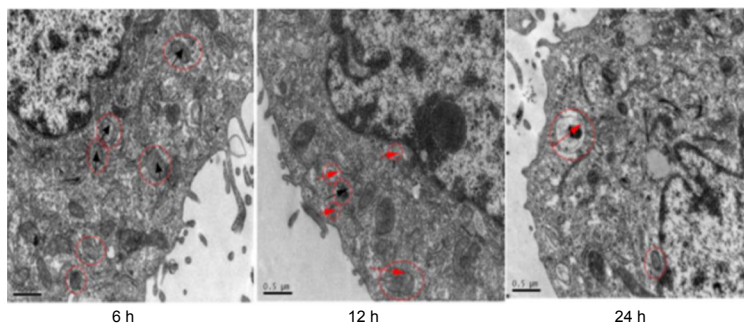

Figure 3 Fetal neural stem cells, observed by transmission electron microscopy, after treatment with 9.56 mM emulsified isoflurane for 6, 12 and 24 hours.
The black arrows indicate autophagosomes, with double-membrane structures, after 6 or 12 hours of emulsified isoflurane treatment. The red arrows show autophagolysosome formation, with monolayer membranes, due to lysosome degradation, in fetal neural stem cells exposed to emulsified isoflurane for 12 or 24 hours. Scale bars: 0.5 μm.

disease, Alzheimer's disease, and Huntington's disease (Carra et al., 2008; Lipinski et al., 2010; Oliver et al., 2019). Thus, autophagy may have a cytoprotective function (Wang et al., 2012; Jiang et al., 2014; Vidoni et al., 2017). Deficient or inhibited autophagy may lead to cell death. The activation of autophagy appears to represent a good strategy for preventing Parkinson's disease progression. Autophagy has also been associated with the pathogenesis of a variety of diseases, such as liver disease, muscle tissue damage, nerve degeneration, and tumors (Czaja et al., 2013; Ghavami et al., 2014).

Our study showed that autophagy increased and mediated caspase-dependent components, following the apoptotic stimulation of FNSCs. Increased autophagosome formation, following the exposure of FNSCs to EI, demonstrated increased autophagic flux. Our results also showed that autophagy inhibition contributed to neuronal apoptosis. The

knockdown of Atg5 aggravated EI-induced apoptosis, which was similar to previous results (Mizushima et al., 2007; Zhao et al., 2013; Huang et al., 2014). FNSC survival was suppressed by Atg5 gene silencing, suggesting that the Atg5 autophagy pathway is strongly associated with the activation of autophagy, following EI exposure.

The detection of LC3 and the determination of autophagosome morphology were performed to measure autophagy. Studies have detected autophagy activity, including autophagosomes and GFP-LC3B fluorescent puncta, in a rat FNSCs model and have evaluated Beclin-1, an important regulator and biomarker of autophagy activity during autophagosome formation (Vicencio et al., 2009; Maiuri et al., 2010; Fernández et al., 2018). Furthermore, autophagy activity may be an upstream regulator of apoptosis, and excessive autophagy can lead to apoptosis-mediated cell death. The overexpres-
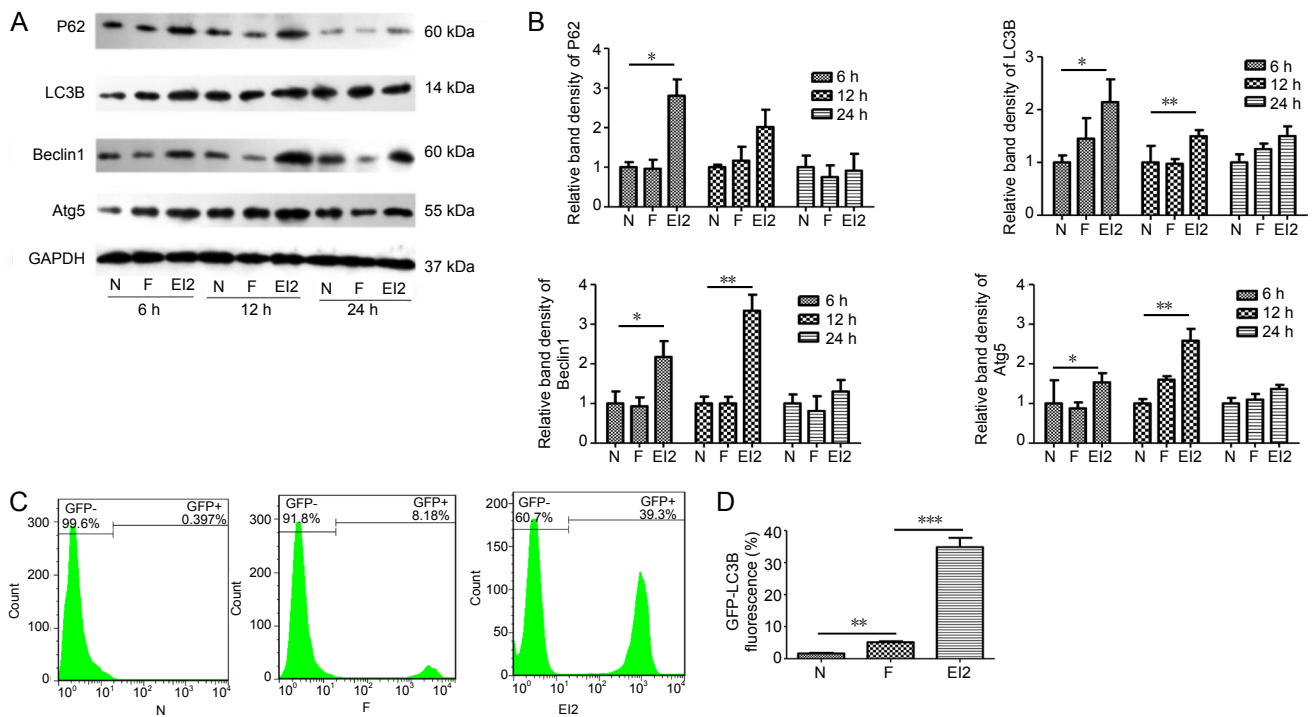
Figure 4 Autophagy-related protein levels and the autophagy flux of fetal neural stem cells after EI treatment.
(A) Western blot assay of the autophagy-related proteins P62, LC3B, Beclin1, and Atg5 after EI treatment for 6, 12 and 24 hours. (B) Expression of autophagy-related proteins compared with that in group N. Representative immunoblots for P62 (A), and the corresponding quantification (B), show that EI treatment for 6 hours significantly increased P62 expression compared with group N. GAPDH was used as a loading control. Values are expressed as a percentage of control. In contrast, the autophagy-related proteins Atg5, LC3B, and Beclin 1 increased dramatically in fetal neural stem cells treated for 12 hours compared with group N. (C and D) GFP-LC3B puncta assay was performed to monitor autophagy flux in fetal neural stem cells. GFP-LC3B-transfected cells were treated with EI for 12 hours and analyzed using flow cytometry. Treatment with 9.52 mM EI (group EI2) significantly enhanced GFP-LC3B puncta compared with group N. All data were derived from the results of three independent experiments. Data are expressed as the mean ± SD ($n = 8$ for each condition; one-way analysis of variance, with Tukey's *post hoc* test). *$P < 0.05$, **$P < 0.01$, ***$P < 0.001$. EI1, EI2, EI3: 7.56, 9.52, 11.48 mM EI groups, respectively; F: Fat emulsion group; N: normal control group. EI: Emulsified isoflurane; GAPDH: glyceraldehyde-3-phosphate dehydrogenase; GFP: green fluorescent protein.
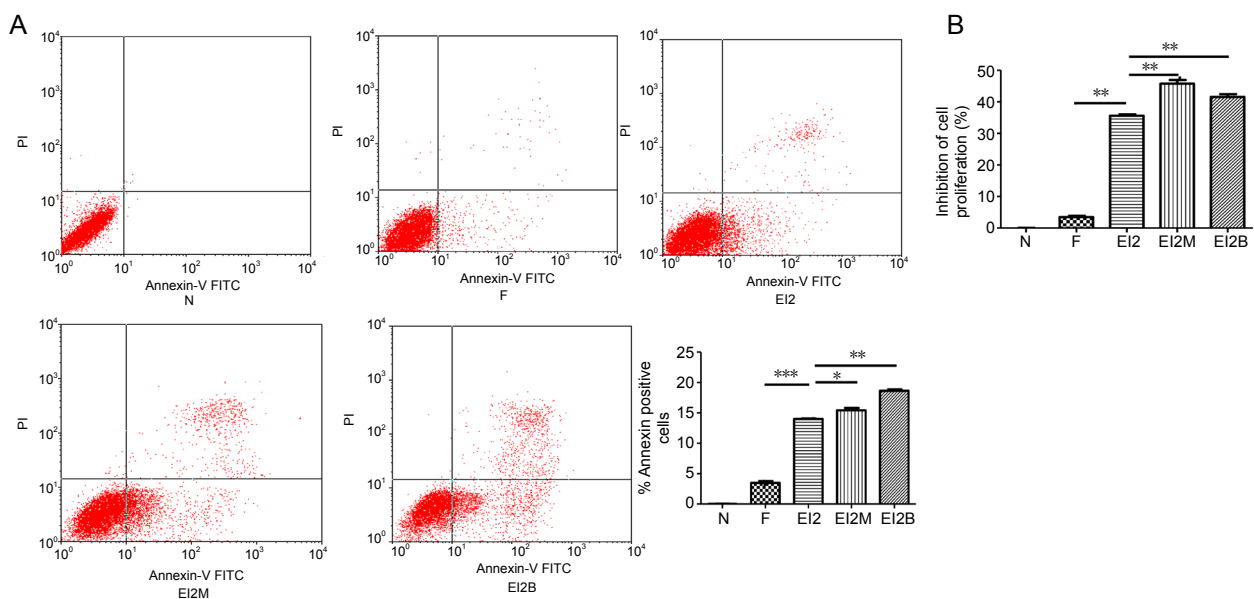

Figure 5 Autophagy inhibition by 3-MA increases EI-induced toxicity in fetal neural stem cells.
(A) Cells were treated with EI, EI plus 3-MA, and EI plus bafilomycin A1 for 12 hours, stained with Annexin V-FITC and PI, and analyzed by flow cytometry. (B) Inhibition of proliferation in groups N, F, EI2, EI2MA, and EI2B. All data were derived from the results of three independent experiments. Data are expressed as the mean ± SD ($n = 8$ for each condition; one-way analysis of variance, with Tukey's *post hoc* test). *$P < 0.05$, **$P < 0.01$, ***$P < 0.001$. EI1, EI2, EI3: 7.56, 9.52, 11.48 mM EI groups, respectively. EI2B: EI2 plus autophagy blocker bafilomycin group; EI2M: EI2 plus autophagy blocker 3-MA group; F: fat emulsion group; N: normal control group. EI: Emulsified isoflurane; FITC: fluorescein isothiocyanate; GAPDH: glyceraldehyde-3-phosphate dehydrogenase; PI: propidium iodide.
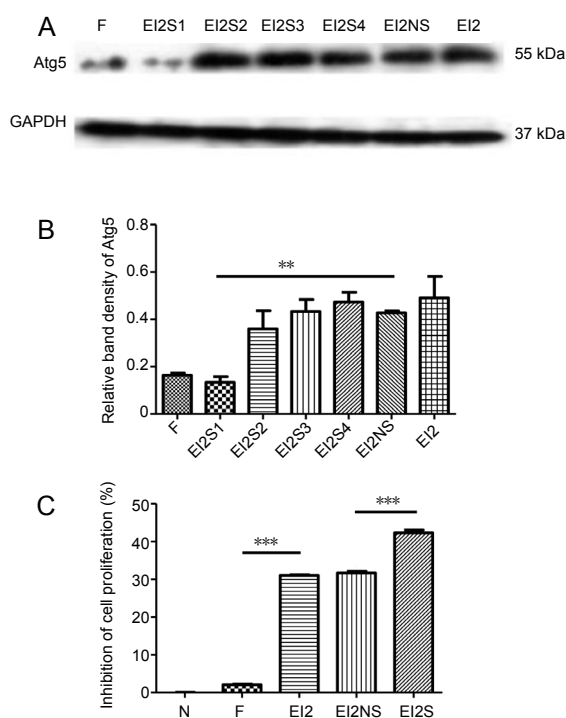
Figure 6 Fetal neural stem cells transfected with siRNA-Atg5 (including siRNA-Atg5-1, siRNA-Atg5-2, siRNA-Atg5-3, siRNA-Atg5-4; and siRNA-Atg5) and treated with 9.80 mM EI (EI2S1, EI2S2, EI2S3, EI2S4, and EI2S5, respectively), to monitor cell apoptosis under autophagy-related gene silencing conditions.
(A and B) Expression of Atg5 protein by western blot assay. (C) Detection of FNSC apoptosis (inhibition of cell proliferation) by MTT assay, following EI treatment under autophagy-related gene silencing conditions. All data were derived from the results of three independent experiments. Data are expressed as the mean ± SD ($n = 8$ for each condition; one-way analysis of variance, with Tukey's *post hoc* test). ∗∗$P < 0.01$, ∗∗∗$P < 0.001$. EI2NS: EI2 plus negative-siRNA group. EI2S: EI2 plus siRNA-Atg5 transfection group; F: fat emulsion group; N: normal control group. EI: Emulsified isoflurane; GAPDH: glyceraldehyde-3-phosphate dehydrogenase; MTT: 3-(4,5-dimethylthiazol-2-yl)-2,5-diphenyltetrazolium bromide.

sion of Beclin-1 has been demonstrated to protect against neural cell death (Rong et al., 2019). Numerous *in vivo* and *in vitro* experiments have demonstrated that isoflurane has a protective effect against many bio-stress conditions, while simultaneously inducing neurotoxicity (Kitano et al., 2007; Zhu et al., 2010b; Wang et al., 2011; Burchell et al., 2013; Wang et al., 2016; Xu et al., 2016; Zhao et al., 2016; Xi et al., 2018).

In this study, concentrations higher than 2.8 mM EI affected FNSC proliferation; however, these concentrations are much higher than those used during clinical applications. We examined the FNSC neurotoxicity induced by exposure to high concentrations of EI, which affects the development and functions of the nervous system, making these cells suitable for studying the mechanisms of anesthetic-induced toxicity on developmental nerves.

In the present study, EI suppressed cell survival and induced apoptosis in FNSCs, in a time- and dose-dependent manner (partial results are shown). Under stress conditions, autophagy provides the necessary nutrients for the maintenance of cellular homeostasis and cellular metabolism and plays a vital prosurvival role (Cao et al., 2016; Yang et al.,

2017).

The present study demonstrated that EI induced Atg5-reliant autophagy in FNSCs. The pharmacological suppression of autophagy decreased FNSC survival following EI exposure. The inhibition of the Atg5 autophagic pathway led to the suppression of cell survival and increased cell apoptosis, and the opposite effects were observed when this pathway was activated, which is consistent with previous results (Kuma et al., 2004). Previous studies also identified an Atg5-independent autophagy pathway (Su et al., 2017; Ye et al., 2018; Duan et al., 2019).

Our study found that the expression of the LC3B-II protein increased after EI treatment. The results demonstrated that autophagy enhancement protected FNSCs against EI-induced toxicity, via the Atg5 pathway. The application of Atg5 gene silencing and the autophagy inhibitor 3-MA reduced FSNC proliferation following EI treatment, suggesting the potential for autophagy inhibition as a neurodegenerative disease therapy. The localization and aggregation of LC3 contribute to autophagosome formation, which is regarded as a conclusive marker of autophagy activation (Bjorkoy et al., 2005).

This study has some limitations. *In vivo* studies are necessary to verify our *in vitro* findings. The potential link between EI-induced FNSC damage and autophagy is a preliminary finding. Thus, we cannot conclude that autophagy regulates EI-induced neural apoptosis in patients. However, we demonstrated a possible link between EI-induced FNSC apoptosis and autophagy, *in vitro*, which warrants further research, *in vivo*.

In summary, EI effectively inhibited cell survival and activated autophagy and apoptosis in FNSCs via the Atg5 signaling pathway, *in vitro*, suggesting that the Atg5 signaling pathway may be used as a therapeutic target for treating neurotoxicity following EI exposure. However, further *in vivo* studies are necessary to determine the EI-induced neurotoxicity mechanism. The stimulation of specific autophagy pathways may represent a new approach for inducing neuroprotection in developmental nerves.

available from the corresponding author on reasonable request.
Plagiarism check: *Checked twice by iThenticate.*
Peer review: *Externally peer reviewed.*
Open access statement: *This is an open access journal, and articles are distributed under the terms of the Creative Commons Attribution-Non-Commercial-ShareAlike 4.0 License, which allows others to remix, tweak, and build upon the work non-commercially, as long as appropriate credit is given and the new creations are licensed under the identical terms.*
Open peer reviewer: *Shreyasi Chatterjee, University of Southampton, USA.*
Additional file: *Open peer review report 1.*

References

Anglade P, Vyas S, Javoy-Agid F, Herrero MT, Michel PP, Marquez J, Prigent AM, Ruberg M, Hirsch EC, Agid Y (1997) Apoptosis and autophagy in nigral neurons of patients with Parkinson's disease. Histol Histopathol 12:25-31.

Bjorkoy G, Lamark T, Brech A, Outzen H, Perander M, Overvatn A, Stenmark H, Johansen T(2005). p62/SQSTM1 forms protein aggregates degraded by autophagy and has a protective effect on huntingtin-induced cell death. J Cell Biol 171:603-614.

Boland B, Kumar A, Lee S, Platt FM, Wegiel J, Yu WH, Nixon RA (2008) Autophagy Induction and autophagosome clearance in neurons: relationship to autophagic pathology in Alzheimer's disease. J Neurosci 28:6926-6937.

Burchell SR, Dixon BJ, Tang J, Zhang JH (2013) Isoflurane provides neuroprotection in neonatal hypoxic ischemic brain injury. J Investig Med 61:1078-1083.

Cao L, Fu M, Kumar S, Kumar A (2016) Methamphetamine potentiates HIV-1 gp120-mediated autophagy via Beclin-1 and Atg5/7 as a pro-survival response in astrocytes. Cell Death Dis 7:e2425.

Carra S, Seguin SJ, Lambert H, Landry J (2008) HspB8 chaperone activity toward poly(Q)-containing proteins depends on its association with Bag3, a stimulator of macroautophagy. J Biol Chem 283:1437-1444.

Cerri S, Blandini F (2019) Role of autophagy in Parkinson's disease. Curr Med Chem 26:3702-3718.

Ciechanover A, Kwon YT (2015) Degradation of misfolded proteins in neurodegenerative diseases: therapeutic targets and strategies. Exp Mol Med 47:e147.

Culley DJ, Baxter MG, Yukhananov R, Crosby G (2004) Long-term impairment of acquisition of a spatial memory task following isoflurane-nitrous oxide anesthesia in rats. Anesthesiology 100:309-314.

Czaja MJ, Ding WX, Donohue TM Jr, Friedman SL, Kim JS, Komatsu M, Lemasters JJ, Lemoine A, Lin JD, Ou JJ, Perlmutter DH, Randall G, Ray RB, Tsung A, Yin XM (2013) Functions of autophagy in normal and diseased liver. Autophagy 9:1131-1158.

Duan X, Liu X, Li W, Holmes JA, Kruger AJ, Yang C, Li Y, Xu M, Ye H, Li S, Liao X, Sheng Q, Chen D, Shao T, Cheng Z, Kaj B, Schaefer EA, Li S, Chen L, Lin W, Chung RT (2019) Microrna-130a downregulates HCV replication through anatg5-dependent autophagy pathway. Cells 8:338.

Fernández ÁF, Sebti S, Wei Y, Zou Z, Shi M, McMillan KL, He C, Ting T, Liu Y, Chiang WC, Marciano DK, Schiattarella GG, Bhagat G, Moe OW, Hu MC, Levine B (2018) Disruption of the beclin 1-BCL2 autophagy regulatory complex promotes longevity in mice. Nature 558:136-140.

Ghavami S, Shojaei S, Yeganeh B, Ande SR, Jangamreddy JR, Mehrpour M, Christoffersson J, Chaabane W, Moghadam AR, Kashani HH, Hashemi M, Owji AA, Łos MJ (2014) Autophagy and apoptosis dysfunction in neurodegenerative disorders. Prog Neurobiol 112:24-49.

Guo F, Liu X, Cai H, Le W (2018) Autophagy in neurodegenerative diseases: pathogenesis and therapy. Brain Pathol 28:3-13.

Huang H, Li R, Liu J, Zhang W, Liao T, Yi X (2014) A phase I, dose-escalation trial evaluating the safety and efficacy of emulsified isoflurane in healthy human volunteers. Anesthesiology 120:614-625.

Istaphanous GK, Ward CG, Nan X (2013) Characterization and quantification of isoflurane-induced developmental apoptotic cell death in mouse cerebral cortex. Anesth Analg 116:845-854.

Jiang T, Yu JT, Zhu XC, Tan MS, Wang HF, Cao L, Zhang QQ, Shi JQ, Gao L, Qin H, Zhang YD, Tan L (2014) Temsirolimus promotes autophagic clearance of amyloid-beta and provides protective effects in cellular and animal models of Alzheimer's disease. Pharmacol Res 81:54-63.

Kalkman CJ, Peelen L, Moons KG, Veenhuizen M, Bruens M, Sinnema G, Jong TP (2009) Behavior and development in children and age at the time of first anesthetic exposure. Anesthesiology 110: 805-812.

Kitano H, Kirsch JR, Hurn PD, Murphy SJ (2007) Inhalational anesthetics as neuroprotectants or chemical preconditioning agents in ischemic brain. J Cereb Blood Flow Metab 27:1108-1128.

Kuma A, Hatano M, Matsui M, Yamamoto A, Nakaya H, Yoshimori T, Ohsumi Y, Tokuhisa T, Mizushima N (2004) The role of autophagy during the early neonatal starvation period. Nature 432:1032-1036.

Levin ER (2009) Plasma membrane estrogen receptors. Trends Endocrinol Metab 20:477-482.

Lipinski MM, Zheng B, Lu T, Yan ZY, Py BF, Ng A, Xavier RJ, Li C, Yankner BA, Scherzer CR, Yuan JY (2010) Genome-wide analysis reveals mechanisms modulating autophagy in normal brain aging and in Alzheimer's disease. Proc Natl Acad Sci U S A 107:14164-14169.

Loepke AW, Istaphanous GK, McAuliffe JJ 3rd, Miles L, Hughes EA, McCann JC, Harlow KE, Kurth CD, Williams MT, Vorhees CV, Danzer SC (2009) The effects of neonatal isoflurane exposure in mice on brain cell viability, adult behavior, learning, and memory. Anesth Analg 108:90-104.

Maiuri MC, Criollo A, Kroemer G (2010) Crosstalk between apoptosis and autophagy within the Beclin 1 interactome. EMBO J 29:515-516.

Menzies FM, Fleming A, Caricasole A, Bento C, Andrews S, Ashkenazi A, Füllgrabe J, Jackson A, Sanchez MJ, Karabiyik C, Licitra F, Ramirez AL, Pavel M, Puri C, Renna M, Ricketts T, Schlotawa L, Vicinanza M, Won H, Zhu Y, Skidmore J, Rubinsztein DC (2017) Autophagy and Neurodegeneration: pathogenic mechanisms and therapeutic opportunities. Neuron 93:1015-1034.

Mizushima N (2007) Autophagy: process and function. Genes Dev 21:2861-2873.

Monk TG, Weldon BC, Garvan CW, Dede DE, Aa MT, Heilman KM, Gravenstein JS (2008) Predictors of cognitive dysfunction after major noncardiac surgery. Anesthesiology 108:18-30.

Oliver D, Reddy PH (2019) Dynamics of dynamin-related protein 1 in Alzheimer's disease and other neurodegenerative diseases. Cells 23:8.

Peng Y, Zheng M, Feng B, Chen XH, Yu BQ, Lu AG, Wang ML, Li JW, Ma JJ, Xu L (2008) Hyperthermic CO_2 pneumoperitoneum induces apoptosis in human colon cancer cells through Bax-associated mitochondrial pathway. Oncol Rep 19:73-79.

Plaza-Zabala A, Sierra-Torre V, Sierra A (2017) Autophagy and microglia: novel partners in neurodegeneration and aging. Int J Mol Sci 18:598.

Switon K, Kotulska K, Janusz-Kaminska A, Zmorzynska J, Jaworski J (2017) Molecular neurobiology of mTOR. Neuroscience 341:112-153.

Rong Y, Liu W, Lv C, Wang J, Luo Y, Jiang D, Li L, Zhou Z, Zhou W, Li Q, Yin G, Yu L, Fan J, Cai W (2019) Neural stem cell small extracellular vesicle-based delivery of 14-3-3t reduces apoptosis and neuroinflammation following traumatic spinal cord injury by enhancing autophagy by targeting Beclin-1. Aging (Albany NY) 11:7723-7745.

Sarkar S, Rubinsztein DC (2008) Huntington's disease: degradation of mutant huntingtin by autophagy. FEBS J 275:4263-4270.

Seong SB, Ha DS, Min SY, Ha TS (2019) Autophagy precedes apoptosis in angiotensin II-induced podocyte injury. Cell Physiol Biochem 53:747-759.

Stratmann G, Sall JW, May LD, Bell JS, Magnusson KR, Rau V, Visrodia KH, Alvi RS, Ku B, Lee MT, Dai R (2009) Isoflurane differentially affects neurogenesis and long-term neurocognitive function in 60-day-old and 7-day-old rats. Anesthesiology 110:834-848.

Su LY, Luo R, Liu Q, Su J, Yang L, Ding Y, Xu L, Yao Y (2017) Atg5- and Atg7-dependent autophagy in dopaminergic neurons regulates cellular and behavioral responses to morphine. Autophagy 13:1496-1511.

Tsujimoto Y, Shimizu S (2005) Another way to die: autophagic programmed cell death. Cell Death Differ 12:1528-1534.

Vicencio JM, Ortiz C, Criollo A, Jones AW, Kepp O, Galluzzi L, Joza N, Vitale I, Morselli E, Tailler M, Castedo M, Maiuri MC, Molgó J, Szabadkai G, Lavandero S, Kroemer G (2009) The inositol 1,4,5-trisphosphate receptor regulates autophagy through its interaction with Beclin 1. Cell Death Differ 16:1006-1017.

Vidoni C, Secomandi E, Castiglioni A, Melone MAB, Isidoro C (2017) Resveratrol protects neuronal-like cells expressing mutant Huntingtin from dopamine toxicity by rescuing ATG4-mediated autophagosome formation. Neurochem Int 117:174-187.

Wang IF, Guo BS, Liu YC, Wu CC, Yang CH, Tsai KJ, Shen CJ (2012) Autophagy activators rescue and alleviate pathogenesis of a mouse model with proteinopathies of the TAR DNA-binding protein 43. Proc Natl Acad Sci U S A 109:15024-15029.

Wang K, Kong X (2016) Isofluranepreconditioning induces neuroprotection by up-regulation of trek1 in a rat model ofspinalcordischemic injury. Biomol Ther (Seoul) 24:495-500.

Wang Q, Liang G, Yang H, Wang S, Eckenhoff MF, Wei H (2011) The common inhaled anesthetic isoflurane increases aggregation of huntingtin and alters calcium homeostasis in a cell model of Huntington's disease. Toxicol Appl Pharmacol 250:291-298.

Wilder RT, Flick RP, Sprung J, Katusic SK, Barbaresi WJ, Mickelson C, Gleich SJ, Schroeder DR, Weaver AL, Warner DO (2009) Early exposure to anesthesia and learning disabilities in a population-based birth cohort. Anesthesiology 110:796-804.

Xi JS, Wang YF, Long XX, Ma Y (2018) Mangiferin potentiates neuroprotection by isoflurane in neonatal hypoxic brain injury by reducing oxidative stress and activation of phosphatidylinositol-3-kinase/Akt/mammalian target of rapamycin (PI3K/Akt/mTOR) signaling. Med Sci Monit 24:7459-7468.

Xu Y, Xue H, Zhao P, Yang YT, Ji GY, Yu WW, Han G, Ding MM, Wang FF (2016) Isoflurane postconditioning induces concentration- and timing-dependent neuroprotection partly mediated by the GluR2 AMPA receptor in neonatal rats after brain hypoxia-ischemia. J Anesth 30:427-436.

Yang B, Zhao S (2017) Polydatin regulates proliferation, apoptosis and autophagy in multiple myeloma cells through mTOR/p70s6k pathway. Onco Targets Ther 16:935-944.

Ye X, Zhou XJ, Zhang H (2018) Exploring the role of autophagy-related gene 5 (ATG5) yields important insights into autophagy in autoimmune/autoinflammatory diseases. Front Immunol 9:2334.

Zhao DA, Bi LY, Huang Q, Zhang FM, Han ZM (2016) Isoflurane provides neuroprotection in neonatal hypoxic ischemic brain injury by suppressing apoptosis. Braz J Anesthesiol 66:613-621.

Zhao X, Yang Z, Liang G, Wu Z, Peng Y, Joseph DJ, Inan S, Wei HF (2013) Dual effects of isoflurane on proliferation, differentiation, and survival in human neuroprogenitor cells. Anesthesiology 118:537-549.

Zhao Y, Liang G, Chen Q, Joseph DJ, Meng QC, Eckenhoff RG, Eckenhoff MF, Wei HF (2010) Anesthetic-induced neurodegeneration mediated via inositol 1,4,5-trisphosphate receptors. J Pharmacol Exp Ther 333:14-22.

Zhu C, Gao J, Karlsson N, Li Q, Zhang Y, Huang ZH, Li HF, Kuhn HG, Blomgren K (2010a) Isoflurane anesthesia induced persistent, progressive memory impairment, caused a loss of neural stem cells, and reduced neurogenesis in young, but not adult, rodents. J Cereb Blood Flow Metab 30:101-1030.

Zhu W, Wang L, Zhang L, Palmateer JM, Libal NL, Hurn PD, Herson PS, Murphy SJ (2010b) Isoflurane preconditioning neuroprotection in experimental focal stroke is androgen-dependent in male mice. Neuroscience 169:758-769.